The Astrophysical Journal, 577:457–463, 2002 September 20
© 2002. The American Astronomical Society. All rights reserved. Printed in U.S.A.

STATISTICAL CORRELATIONS BETWEEN SOLAR MICROWAVE BURSTS AND CORONAL MASS EJECTIONS

Brian L. Dougherty, Harold Zirin, and Kathryn Hsu
California Institute of Technology, MC 264-33, Pasadena, CA 91125; bld@caltech.edu
Received 2002 March 7; accepted 2002 May 28

ABSTRACT

We compare listings of coronal mass ejections (CMEs) observed by LASCO on *SOHO* and solar microwave bursts (SMBs) recorded by the Radio Solar Telescope Network (RSTN) operated by the United States Air Force. These data sets are the product of stable and continuous observations of the whole Sun and provide suitable bases for robust statistical studies. In total, 3557 coronal ejections and nearly 1051 bursts above 50 sfu were observed from 1996 January through 2001 May. Correlated events are easily distinguished by time proximity. Correlations improve as CME launch heights are projected to the solar limb, when the rms scatter in CME-SMB delay was as little as 16 minutes, but because coronal disturbances are only visible when they emerge from behind occulting disks, timing associations depend on the assumed source and acceleration. The probability of correlation rises with burst flux, duration or temporal complexity, and ejection speed or width. For the 164 SMBs with intensities over 500 sfu, $70\% \pm 8\%$ were associated with CMEs. For the 160 CMEs that were halo-like or have speeds over 1000 km s^{-1} (characteristics that have been associated with geoeffective events), $60\% \pm 8\%$ and $84\% \pm 10\%$ were associated with SMBs, respectively.

Subject headings: Sun: activity — Sun: corona — Sun: coronal mass ejections (CMEs) — Sun: radio radiation

1. INTRODUCTION

Coronal mass ejections (CMEs) are important factors in many "space weather" events affecting the near-Earth environment. Although CMEs may be seen leaving the Sun, it would be desirable to find other solar phenomena that predict or at least accompany their appearance. While it was argued (Gosling 1993) that flares do not play a central role in this regard, later studies found that impulsive, fast or halo-like CMEs, which are now thought to be most geoeffective, are typically accompanied by surface activity (e.g., Brueckner et al. 1998; Hudson et al. 1998; Kocharov et al. 2001). Straightforward statistical comparisons are needed, using samples that overview whole classes of phenomena, to provide firm bases for further study and bounds on theory (Hudson & Cliver 2001).

In this paper we compare large numbers of contemporaneous solar microwave bursts (SMBs) and CMEs. The relationship between these phenomena has received relatively limited treatment in recent literature. The published research is often limited to close examination of a few events. This is a basic study, establishing connections between these two eruptive manifestations before considering other types of solar activity.

Most SMBs start suddenly and almost simultaneously at frequencies from 2 to beyond 20 GHz, peak rapidly, and last a few minutes (Kundu 1965). Bursts with intensities above 1000 sfu are less frequent, as are those lasting an hour or more or extended events that peak several times. SMBs are typically smooth and broadband, predominantly as a result of incoherent gyrosynchrotron radiation, at harmonics of 10–100 from 30–300 keV electrons spiraling in the 300–1000 G magnetic fields of the low corona (Holt & Ramaty 1969; Bastian et al. 1998). We have often found that their spectra vary little throughout each event, with peaks in the 5–10 GHz range. SMBs are well correlated temporally and spatially with hard X-ray flares (Marsh & Hurford 1982; Dulk 1985), since a shared, suddenly energized and/or injected nonthermal electron population is responsible for both (Gary 1985; Lu & Petrosian 1989; Kundu et al. 1994). Neupert (1968) found that they often presage soft X-ray emissions, which follow the thermalization of that source population. SMBs have also been associated with Hα flares, type II and III radio bursts, and interplanetary energetic particle events (Chertok 1982; Vrsnak et al. 1995; Bastian et al. 1998).

CMEs involve large-scale disruptions of coronal magnetic fields and plasmas, often visible in the K corona as expanding loops or sprays (Low 1996; Gopalswamy & Thompson 2000). Their apparent sizes (projected on the sky) subtend a median angular span of about 50°. A few CMEs appear to extend completely around the solar disk and so are called halo events. Apparent speeds can exceed 1000 km s^{-1}, but the median is around 400 km s^{-1}, and there is a dearth of events slower than 100 km s^{-1}. The energies involved range from 10^{31} to 10^{32} ergs in work done to expel 10^{15}–10^{16} g of plasma. Geomagnetic storms are often preceded by faster and/or halo-like CMEs (Brueckner et al. 1998; Cane 2000; St. Cyr et al. 2000; Webb 2000; Kocharov et al. 2001). Their linkages with long-wavelength radio emissions, prominence eruptions, and flares have been studied by various authors (e.g., Gosling et al. 1976; Munro et al. 1979; Sheeley et al. 1983; Robinson & Stewart 1985; Robinson et al. 1986; Gergeley 1986; Cane et al. 1987; Webb & Hundhausen 1987; Harrison et al. 1990; St. Cyr & Webb 1991; Cliver et al. 1999; Gilbert 2000). Faster CMEs are more frequently associated with flares, and slower but accelerating CMEs with eruptive prominences, although the latter are not generally correlated with SMBs (MacQueen & Fisher 1983; Delannee et al. 2000; Andrews & Howard

2001). Long-duration soft X-ray flares and CMEs are linked (Sheeley et al. 1983; Kahler 1989), as are microwave bursts of the gradual rise and fall type or with extended postburst increases (Sheeley et al. 1975).

The duty cycle of SMB observations is almost total, clouds do not interfere, and the events are easily detected by the worldwide Radio Solar Telescope Network (RSTN) and a number of other ground-based instruments. The measured fluxes generally agree between different observatories; typical discrepancies are less than 20%. CMEs are easily observed by a satellite telescope and are visible for some time, and observations are complete for events that are bright enough. One important difficulty arises from the different thresholds for observing these two phenomena. The RSTN record only extends down to 50 sfu, and no uniform assessment of the intensity of CMEs is available. In addition, SMBs on the back side of our Sun are only detected within roughly 10° of longitude around the limb, whereas a large fraction of back-side CMEs are seen. SMBs are uniformly detectable across the solar disk, whereas CME visibility generally falls for events originating around Sun center (Webb & Howard 1994).

There is evidence that many CMEs launch from the low corona (St. Cyr et al. 1999; Delannee et al. 2000), but relatively few imaging data are available to investigate the spatial relationships between bursts and ejections. CMEs and flares are often closely correlated in time, however (Harrison 1995), and most studies matching SMBs and CMEs are based primarily on timing correlations. Chertok et al. (1991) considered 60 Solwind CMEs identified with near-limb flares by other investigators and reported that the coincident SMBs were more intense and lasted longer (especially for CMEs with large angular size) when compared to 20 unassociated bursts. They also found, among those coincident SMBs, that bursts with softer radio spectra were longer lasting, but no control comparisons were made of spectra from unassociated SMBs spanning similar durations (Chertok & Gnezdilov 1993).

For this paper we sought statistically robust correlations through a survey that avoids the introduction of any peculiarities that may result from the study of episodic or selected events. We therefore bypassed data from instruments with limited duty cycle or fields of view, even if several such apparatuses were operated in concert to more comprehensively examine occasional events. There exist other instruments that observe the whole Sun and run independently at rapid cadence with high duty cycle over extended periods. Our study derives from the availability of two large, modern databases resulting from the latter approach. Stable, consistently calibrated measurements were taken, providing several years of overlapping and nearly continuous observations.

We begin by establishing the best correlators, keying on CME versus SMB timing distributions. Next, we extrapolate the launch of CMEs to different heights above the solar limb and mark SMBs with respect to their start or peak times. We then study fluxes, durations, speeds, etc., to distinguish other correlated aspects of these phenomena.

2. DATA

The CMEs of this study were recorded by the Large Angle and Spectrometric Coronagraph Experiment (LASCO) on the *Solar and Heliospheric Observatory* (*SOHO*; Brueckner et al. 1995). A continuously updated catalog of events is available on the World Wide Web, where CMEs dating from 1996 January are listed.[1] Except during 1998 July–1999 February, when the spacecraft was operationally lost, no large gaps in coverage occurred. Shorter outages for regularly scheduled maintenance activity and infrequent corrective actions have been taken into account.

These listings reduce measurements from LASCO coronagraphs C2 and C3, with fields of view extending from 1 to 30 $R_\odot$ beyond the solar limb and at image-taking cadences of 12–36 minutes. Data for each CME include the time at first appearance (usually within C2 images, in Universal Time), solar position angle, angular span, and linear and quadratic fits to height-time plots (i.e., assuming constant speed or acceleration). Also provided are onset times as projected to the solar limb via first- and second-order extrapolations of the corresponding fits.[2] Such projections refer to the leading edges of CMEs, where discernible, not to any nested features. Morphological or brightness differences among CMEs are not noted. Since motion toward or away from Earth cannot be sensed in coronagraph images, the fitted speeds and accelerations relate to apparent movement, projected on the sky plane.

Data quality appears to be uniform throughout this catalog. Individual records are occasionally appended with notes of measurement difficulties or limited coverage, e.g., "only two points" available for fitting. The LASCO collaboration has performed consistency checks and reports that errors are maintained to within 10%. Other LASCO studies suggest that linear height-time fits may be preferable to quadratic fits for most events (St. Cyr et al. 2000). On-line coronagraphic images are available and could be used to reassess certain measurements, but to avoid introducing errors of ignorance or bias, we have taken LASCO results as supplied.

There are 3741 CMEs listed through 2001 May. For this study, we consider only those 3557 events for which a reasonable first-order speed could be found; the remaining 184 were indistinct, seen in only one image, or otherwise badly fitted. The rate of events rose by about a factor of 10 during the current solar cycle. A little more than three CMEs per day have occurred for the last two full years of data.

Listings of microwave bursts were acquired from the National Geophysical Data Center.[3] Included are records from the RSTN, a set of dedicated linearly polarized radiometers tuned to the fixed frequencies of 1415, 2695, 4995, 8800, and 15,400 MHz, among others. These instruments are maintained and operated by the United States Air Force (USAF) and located at four sites around the Earth to provide continuous, 24 hr solar coverage. At the time of writing, listings were available beginning in 1989 through 2001 May. For the present work, we ignored bursts observed when LASCO was otherwise engaged. The total, overlapping CME-SMB live time for this study was therefore 1631 days.

Each RSTN record contains start and peak times, burst durations, peak fluxes, and rough spectral-temporal event–

[1] See http://cdaw.gsfc.nasa.gov/CME_list.
[2] Courtesy of Seiji Yoshiro at GFSC.
[3] See ftp://ftp.ngdc.noaa.gov/STP/SOLAR_DATA/SOLAR_RADIO/BURSTS.

type characterizations. Various data qualifiers are also provided to indicate the status of these records (e.g., preliminary, uncertain, corrected, final) or observing conditions (poor to excellent). Start times mark those moments when the intensity for at least one frequency first crosses certain thresholds, typically 50 sfu (1 sfu $= 10^{-22}$ W m^{-2} Hz^{-1}). Lower intensity measurements from other frequencies are occasionally reported, but the USAF has maintained no uniform requirement to do so. The USAF does regularly compare quiet-Sun flux measurements to ensure common calibrations among all observing stations.

Limiting the selection of listings of RSTN data yields 6253 records. Many of these refer to the same events observed at different frequencies and/or from more than one site. To distinguish individual bursts, we grouped records with start times that fell between the start and peak times of others. We then imposed a 50 sfu peak threshold to avoid effects from the nonuniform reporting of smaller events. A total of 1051 bursts were found using this algorithm, most of which took place during the last two years of the current solar cycle. An uncertainty of ± 34 events had to be assessed, as a result of the 1 minute granularity of USAF records. Since the sampling rate of RSTN radiometers is much higher than this, further timing ambiguities are unlikely. Each event found therefore represents a distinct brightening of microwave output from our Sun.

Since observable SMBs must appear on or near the front side of our Sun, the actual number of bursts that occurred may be nearly twice this sum. In addition, we find that the number of SMBs per flux interval (measured in sfu) falls as $dN/dF \approx 29,200F^{-(1.92\pm0.10)}$, consistent with that determined elsewhere (Nita et al. 2002). The burst total could rise by a factor of 8 if detection thresholds were dropped to around 5 sfu; i.e., well over 10,000 SMBs may have actually transpired, of which RSTN reported only the larger events.

To check RSTN coverage, we plotted the apparent rate of SMBs occurring in each hour of the day for several years. A flat rate, with no diurnal features, confirms a uniform duty cycle. LASCO records reveal a similar uniformity.

3. TIMING CORRELATIONS

Since spatial information is lacking in the LASCO and RSTN databases, our primary means of finding related events is by noting time delays between these two phenomena. Consider the peak time of each SMB (i.e., that moment of maximum intensity for whichever frequency had the highest flux) and first-appearance times of the CMEs. These are not the timing marks we will find later to be most significant, but they serve here to illustrate our procedure. For each of the 1051 RSTN bursts identified, we searched LASCO data for the nearest ejection, regardless of whether it occurred earlier or later, and plotted the distribution of time intervals (Fig. 1*b*).

Unique associations are not required here. Occasionally, more than one burst may occur near a common CME. Series of SMBs do sometimes happen, but we need not be concerned about double-counting such events. We seek correlations between CMEs and distinct enhancements of solar microwave intensity, regardless of whether the latter are part of a group of bursts.

The peak, centered around 30 minutes, indicates that some CMEs and SMBs are correlated, with ejections becoming visible within LASCO coronagraphs about a half-hour after the associated radio bursts reach their intensity maxima. This peak extends above a random background of accidental pairings, which spans the entire time window. To estimate that distribution of accidental coincidences, we randomized SMB times within each catalog month and repeated the above procedure, resulting in Figure 1*a*. As expected, a symmetrical, double-sided exponential curve fits the latter distribution quite well. The mean fore-aft time delay is 160 minutes. (To understand this fall-off behavior, consider that in any random process, for the very next event to appear N minutes after any given time mark, there must occur no intervening events during the previous $N - 1$ minutes, a happenstance that becomes progressively unlikely as N increases.)

Exponentials with the same time constant are then fitted along with a Gaussian curve to the delays in the actual data of Figure 1*b*. The number of correlated events indicated (within the Gaussian only, above accidental backgrounds) is 423 ± 28. The most probable delay between linked CMEs

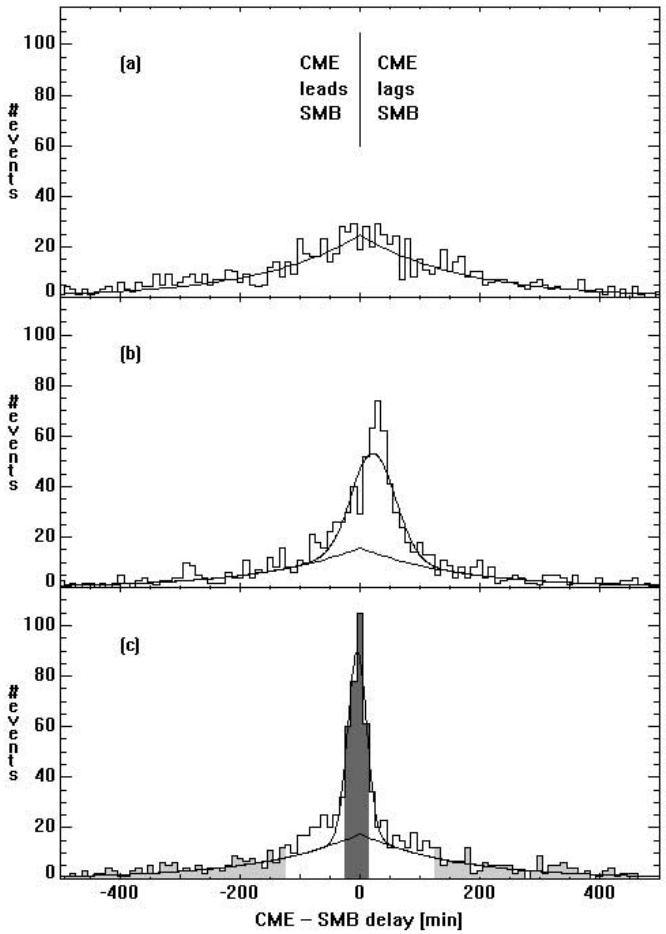

FIG. 1.—Distribution of time intervals between each SMB and the nearest CME, regardless of whether the latter precede or follow. The bins are 10 minutes wide. Fitted curves include two-sided exponentials (centered at zero) below free-floating Gaussians. (*a*) SMB times were artificially randomized within each month, to present a distribution of uncorrelated events. (*b*) CME times were taken at first appearance in the LASCO C2 coronagraph, while SMB times were taken at the moment of peak intensity among all observed frequencies for each event. (*c*) CME onsets were projected to the solar limb via second-order extrapolations, to account for acceleration. There are equal numbers of events represented in the dark gray (largely correlated) and light gray (uncorrelated) areas. Data from events in these latter timing ranges are plotted as filled and unfilled symbols in Fig. 3.

and SMBs is 31 minutes, with ejections following bursts. The rms scatter (Gaussian width) among these events is 36 minutes, in part as a result of the coarseness of C2 cadences. Beyond this Gaussian, a good exponential fit suggests that there are no other associated CME-SMB pairings.

A 31 minute delay is consistent with disturbances traveling around 500 km s^{-1} (representative of CME speeds) rising from the solar limb to nearly 1.4 $R_{\odot}$ above it (i.e., just beyond the C2 mask edge, and roughly typical of first-appearance heights). This plainly suggests a common CME-SMB origin in the lower corona. If we repeat our timing comparisons, only now projecting CME onsets to the solar limb (via quadratic extrapolations to account for measured accelerations), then Figure 1*c* results. The Gaussian is narrower (with an rms width of 16 minutes) yet contains a similar excess of events (396 ± 28). Its position, centered at -3.5 minutes, implies little delay between events.

We now project CME onsets to various heights in the corona. Both first- and second-order extrapolations are compared (Fig. 2). We also check for differences that result when radio bursts are timed with respect to their starts instead of their peaks. (To establish SMB start times, we first found which RSTN frequency was observed with the highest flux overall for that event, then used its reported threshold-crossing time.) The least scatter in correlated time delays occurs when CMEs are projected via second-order extrapolations to the solar limb. Curves at the top of Figure 2 follow the rms widths of our fitted Gaussians, with filled and open symbols designating SMB start and peak times, respectively, and squares and circles designating second- and first-order CME projections, respectively. To avoid confusion, error bars and quadratic fits to these results are provided for filled symbols only.

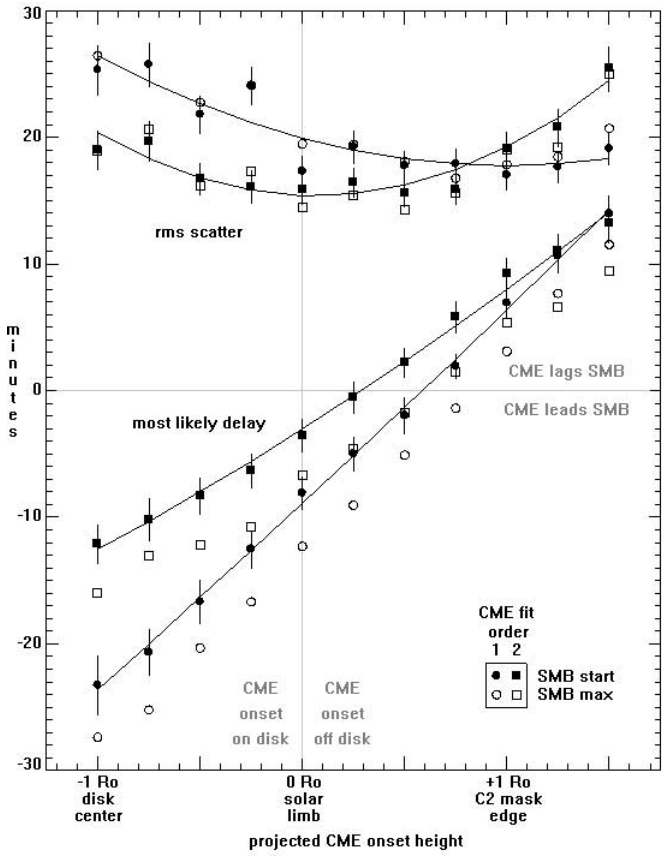

FIG. 2.—*Upper symbols:* rms scatter for time intervals between correlated CME and SMB events. *Lower symbols:* Most probable delays between correlated CMEs and SMBs. Squares (circles) indicate extrapolations of CME launch times, assuming constant acceleration (velocity). Open (filled) symbols designate SMB peak (start) times. Error bars and quadratic curve fits are shown for filled symbols only.

In separate analyses, we found that correlated CME-SMB timing scatter increased slightly when each RSTN listing was treated independently, as if all 6253 records marked different bursts. At an alternate extreme, we tried grouping RSTN records whose start times fell between the start and end times (instead of peak times) of other records and found that scatter in CME-SMB delays became slightly smaller. Neither effect was statistically significant. In both cases, we timed SMBs with respect to their starts and projected CME launches to the solar surface. Except for the multiplicity of bursts assumed, it did not matter to our timing results how individual radio bursts were distinguished.

The lower curves of Figure 2 track the most probable delays between associated SMBs and CMEs. It would appear that limb-projected CMEs lead SMBs by a few minutes. This is consistent with earlier studies (e.g., see Harrison et al. 1990 for comparisons with soft X-ray flares), but as seen in the figure, delays change markedly when SMB start or peak times are used or when first- or second-order CME extrapolations are followed. CMEs that are projected to the limb without accounting for acceleration lead their correlated SMB peak times by just over 12 minutes on average, whereas the use of second-order projections and the threshold-crossing times of bursts decreases this lead to just 3.5 minutes. Moreover, correlated bursts tend to peak roughly 4 minutes after crossing thresholds, but the use of true start times would further reduce this delay. (More study is needed on this last point, possibly involving non-RSTN data.)

We note that the use of CME speeds as measured on the sky plane automatically corrects for possible components of motion toward or away from Earth. We also note that CME launch-time errors would be expected to increase with the distance extrapolated, but the solar limb–to–C2 mask edge distance is only about 3% of the range (29 $R_{\odot}$) over which CMEs are imaged by LASCO. Therefore, the minimum timing scatter of projected CMEs suggests that ejections (or influences that lead to them) actually do originate near the solar surface, not far out in the corona.

Over 91% of LASCO CMEs intersect the Sun's face when quadratic height-time extrapolations are followed. The rest have speeds that project to zero farther out in the corona. Looked at separately, we find only a hint of any relationship between the latter ejections and bursts. On the other hand, linear projections always reach the limb, but Figure 2 shows that such extrapolations tend to be worse: the timing scatter increases when accelerations are neglected.

Correlated events are therefore best distinguished by relating SMBs with CME onsets projected to the solar limb. No assumptions have been made as to cause and effect, and no particular model was used. Smaller timing scatter may indicate that CMEs actually launch from near the solar surface, and delayed SMB start times may obviate suggestions that SMBs initiate CMEs. For the moment, however, we have merely sought an empirical means of discerning linked events.

In general, the number of correlated CME-SMB pairings changed little with different choices of timing parameters

and projected heights. We conclude that roughly 400 events are associated overall, or just over 10% of LASCO CMEs and about 40% of RSTN SMBs. Since nearly half of all visible ejections probably occur on the far side of the Sun, where any associated radio bursts would not be seen, we should double the fraction for CMEs. In any case, these rates are surely dependent on instrumental sensitivities and event characteristics. We will explore the latter issue next.

3.1. *Further Correlations*

Within a window of −25 to 15 minutes in Figure 1*c* (*dark gray region*) there are 308 event pairs, around 237 of which are nonrandomly associated. This is a nearly 80% pure sample, comprising around 60% of all correlated events. For comparison, there are 302 accidental pairings with delays earlier or later than 125 minutes (in the light gray areas). Both of these samples are plotted together in Figure 3.

Correlated SMBs tend to be more intense and last longer than unassociated bursts, while correlated CMEs tend to be wider and faster. Indeed, that portion of Figure 3*a* beyond 10 minutes and above 1000 sfu is almost entirely populated with bursts from the purified sample. When compared to Figures 3*b* and 3*c*, most of these are in turn linked with faster and halo-like CMEs.

A further distinction is seen among the colors of our data points, where radio burst types are indicated. These designations are assigned by RSTN observing stations, based on the following criteria. A typical burst (*black*) peaks only once but can be quite intense. "Gradual rise and fall" bursts (*blue*) are infrequent, take longer to develop, and usually display quite broad, smooth, and weak spectra. "Complex" bursts (*red*) contain significant temporal structure, often peaking several times. For this figure, the most dynamic behavior is plotted, from among all the observed frequencies in each event. It would appear that complex bursts are prone to be associated with CMEs.

In Figure 4*a* we selected from the RSTN database those bursts with peak fluxes in three ranges: 50–500, 500–5000, and above 5000 sfu. (These break points correspond to USAF thresholds for drawing distinctions among bursts of different levels of importance.) There are 888, 133, and 31 such events, respectively, comprising 84%, 13%, and 3% of all SMBs above 50 sfu, as shown by the dashed histogram. We then fit CME-SMB time interval distributions as done for Figure 1*c*, relating those selected bursts to ejections. There are around 286, 90, and 24 linked events in the successive flux increments. Correlation probabilities in each range are shown by the solid histogram, with statistical error bars attached. Summing the last two bins, we find that 70% ± 8% of all bursts with fluxes over 500 sfu are associated with CMEs.

In Figure 4*b* we selected LASCO CMEs with speeds of 100–300, 300–1000, and above 1000 km s^{-1}. We then correlated these ejections with SMBs, as above. There are 922, 2441, and 159 events in each increment, of which nearly 42, 300, and 133 are correlated with bursts. Statistical fluctuations account for any apparent discrepancy in the total number of linked events in Figures 4*a* and 4*b*. We find that only 4.5% of all CMEs have speeds over 1000 km s^{-1}, and 84% ± 10% of those are associated with SMB activity.

In Figure 4*c* we selected LASCO CMEs with angular spans in successive 100° increments. Note that there are more halo-like CMEs than would be expected from the rapidly falling numbers of events with smaller widths. There are 2928, 426, 43, and 160 CMEs in each increment, of which around 265, 100, 24, and 96 were found to be correlated with bursts. Only about 4.5% of all CMEs are halo-like, and 60% ± 8% of those are linked with SMBs.

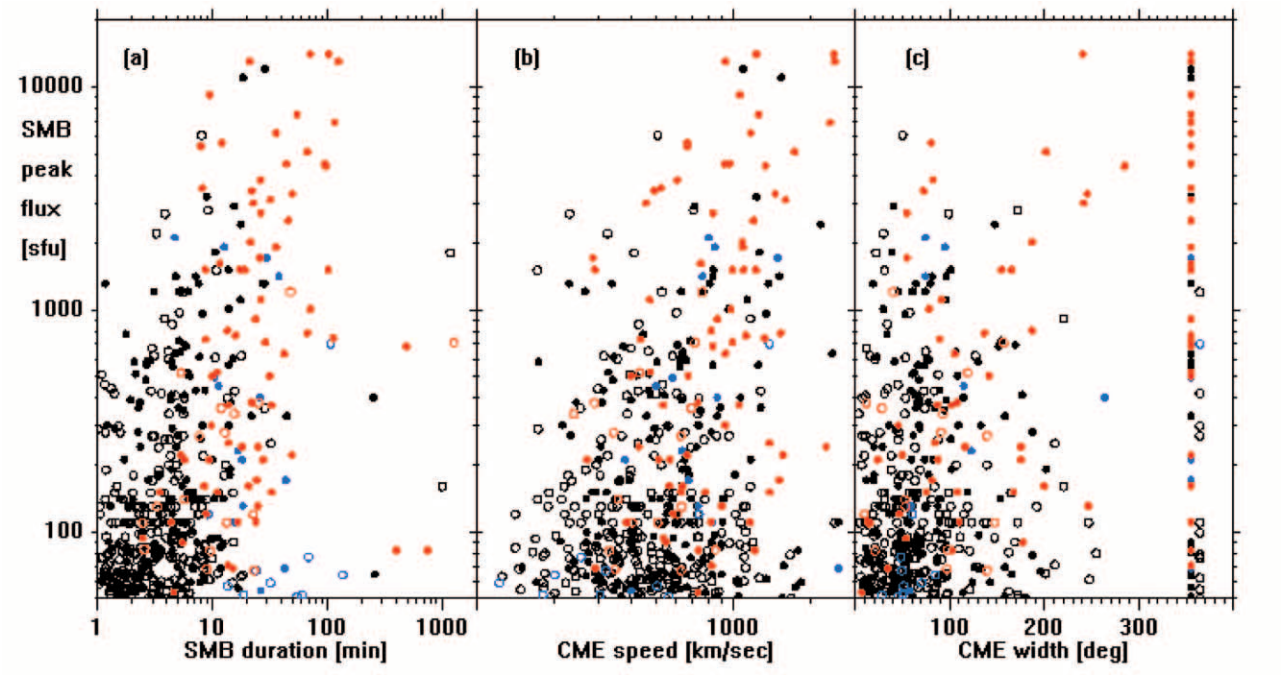

FIG. 3.—Scatter plots of various characteristics for events in which CMEs occur within −25 to 15 minutes of SMBs (*filled circles*) and for an equal number of events that occur 125–500 minutes apart (*open circles*). Peak SMB intensity is plotted vs. (*a*) burst duration, (*b*) CME speed, and (*c*) CME width. Burst type, as assigned by the USAF, is indicated by color: simple, uncomplicated SMBs are in black, gradual rise and fall bursts are in blue, and complex bursts are in red. The columns of events in (*c*) with 360° widths indicate halo CMEs, where filled and open symbols have been separated for ease of viewing.

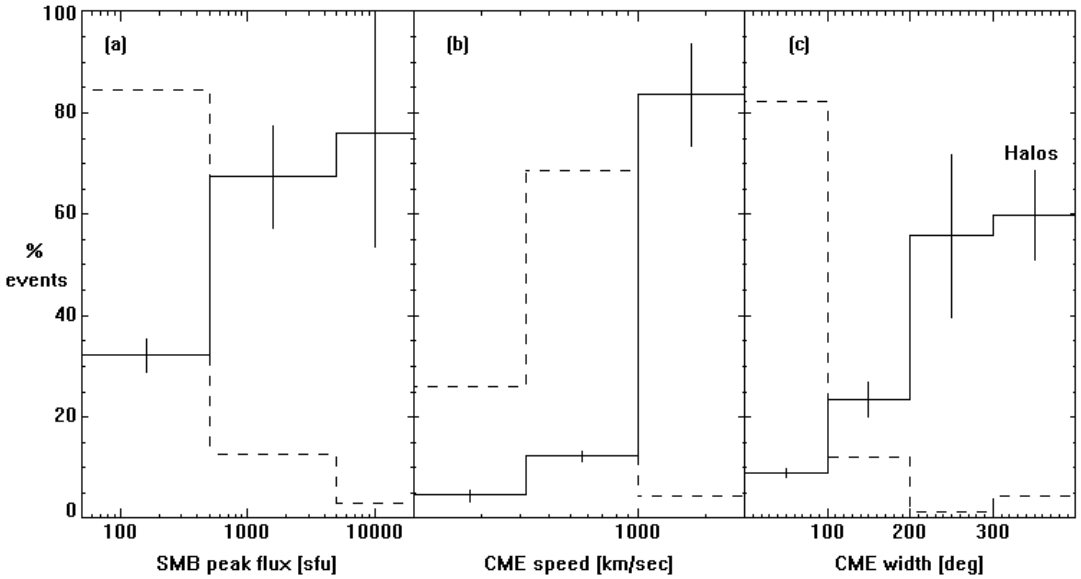

FIG. 4.—*Dashed histograms:* Percentage of all recorded events within each bin. *Solid histograms with error bars:* Percentage of correlated events among the number in each particular bin. (*a*) For SMBs with different peak intensities. (*b*) For CMEs with different speeds. (*c*) For CMEs with different angular spans.

Focusing on the most highly correlated characteristics, there are nearly 100 linked events in which SMB intensities exceed 500 sfu and CME speeds are above 300 km s^{-1}. For those pairings, the most likely CME launch time (projected to the solar limb) leads SMB start times by only about half a minute, and the rms timing scatter is around 14 minutes. In other words, it cannot be determined which began first.

4. DISCUSSION

To our knowledge, LASCO and RSTN databases are the largest to have been searched for relationships between CMEs and SMBs. The straightforward survey presented here provides firm correlations and bases for further studies.

Correlated events were clearly distinguished by time proximity. Second-order extrapolations provide the best means to track CMEs, taking account of accelerations as fitted from height-time plots of leading edges. Such projections yield a timing relationship between CMEs and SMB start times reasonably well described as Gaussian, with an rms scatter around 16 minutes. This relationship is largely insensitive to the ways individual SMBs may be distinguished. The timing scatter between correlated SMBs and CMEs tightens as the latter are projected to launch near the solar surface, consistent with a common origin in space. The actual delay is contingent on whether CMEs accelerate explosively or gradually.

Correlated SMBs tend to be more intense and last longer, while correlated CMEs tend to be faster and wider; 70% of all bursts with fluxes over 500 sfu are associated with CMEs. However, not all correlators are merely size or power related and so subject to the criticism that big eruptions have multiple effects regardless of the detailed physics (Kahler 1982). Correlated SMBs tend to be complex, with multiple temporal maxima.

Definite associations between CMEs and SMBs cannot be made without high-cadence images of coronal ejections observed closer to the solar surface. CMEs probably do not launch with constant velocity, but the occulting disks in LASCO hide both their source and early speed. Certain ejection onset-time proxies may be entertained (e.g., Moreton or EIT waves; see Moreton & Ramsey 1960; Moses et al. 1997), but a one-to-one correspondence has not been established between these phenomena and CMEs, and the observing cadences are low. Similarly, the starting heights of type II bursts, which probably are associated, are not precisely known.

Correlations should also improve if SMB sources were included in our analysis, but RSTN radiometers do not locate bursts. Imaging data should be available, since most flares are recorded in Hα, and virtually all SMBs accompany flares. Alternatively, a new, dedicated instrument capable of measuring both the location and evolving spectra of SMBs anywhere on the solar disk will soon be operational: the Solar Radio Burst Locator (SRBL; Dougherty et al. 2000). Several of the most significant bursts of the past few years have been recorded by a prototype at Caltech's Owens Valley Radio Observatory.[4]

Because RSTN data do not include all (or even most) SMBs with intensities below 50 sfu, it is possible that more, presently uncorrelated CMEs could be paired with smaller bursts. Suppose, as suggested earlier, that over 10,000 SMBs actually occurred with fluxes above 5 sfu during the 1631 days included in this study. Following the trend in Figure 4*a* that the correlation probability falls for weaker bursts, we might guess that roughly 10% of these added SMBs are linked. If that number is doubled to account for unseen, back-side SMBs, then most CMEs may well be associated with microwave bursts. Further study is clearly needed, and SRBL data could provide the basis for that effort.

As SMB intensity rises, so does the rate of correlation with CMEs. Nevertheless, 30% of bursts over 500 sfu are apparently unaccompanied by ejections. This could be an effect of observability as a function of source longitude:

[4] See http://srbl.caltech.edu.

CMEs originating near the limb are more easily detected (Webb & Howard 1994). In addition, coronagraph efficiencies cannot be 100% since an occulting disk is unavoidable and small amounts of mass may be ejected. On the other hand, there may exist a class of large confined bursts. Cliver et al. (1985) have previously noted that big SMBs, especially ones with certain spectral characteristics, could occur without accompanying type II/IV manifestations. Those events may also lack CMEs. Cross-correlating unassociated SMBs with Hα or ultraviolet data, in part to ascertain source locations, may probe both CME detectability and the inevitability of extensive coronal disturbances. Such studies are beyond the limited aims of this paper, but the interesting possibilities mentioned here provide impetus for immediate follow-on investigations.

Ignoring statistical uncertainties, why are more than half of all halo CMEs associated with microwave bursts? If front-side and back-side CMEs were equally detectable, then fractions closer to 50% should be found. But as Andrews (2002) has recently calculated, an asymmetrical visibility relationship is expected, favoring front-side ejections, and this by itself could explain our result.

What about the even more lopsided correlation of fast CMEs with bursts? It is, of course, quite plausible that energetic events and fast CMEs are connected. Other factors enhance this effect: limb CMEs are visible for a sizable longitude range, sky-plane events will obviously display higher velocities, and Andrews' findings still hold. Thus, the apparent sources of fast CMEs may be significantly biased toward the limbs, with front-side events slightly favored in the LASCO data set. In addition, microwaves are known to appear from loop tops at altitudes of 10^4 km, and emissions at much greater heights have not been ruled out, making back-side SMBs visible at least 10° in longitude around the limbs. Altogether, if all fast CMEs were associated with microwave activity, then many more than half of them might be observed to be so.

Halo-like CMEs occur at rates well in excess of expectation if the rates of smaller ejections are extrapolated to wider angular sizes. These CMEs are closely associated with SMBs and appear to expand somewhat faster than typical ejections. Since fast, halo CMEs are particularly geoeffective, it would seem that large, complex SMBs may serve as proxies for certain types of Earth-directed disturbances.

This work was supported by USAF contract F19628-93-C-0013. We thank Seiji Yashiro at GFSC for providing projected CME launch times. The LASCO CME catalog is generated and maintained by the Center for Solar Physics and Space Weather, Catholic University of America, in cooperation with the Naval Research Laboratory and NASA. *SOHO* is a project of international cooperation between ESA and NASA. We also thank the referee for several comments leading to a clearer, stronger submission.

REFERENCES

Andrews, M. D. 2002, Sol. Phys., in press
Andrews, M. D., & Howard, R. A. 2001, Space Sci. Rev., 95, 147
Bastian, T. S., et al. 1998, ARA&A, 36, 131
Brueckner, G. E., et al. 1995, Sol. Phys., 162, 357
———. 1998, Geophys. Res. Lett., 25, 3019
Cane, H. V. 2000, Geophys. Res. Lett., 27, 3591
Cane, H. V., et al. 1987, J. Geophys. Res., 92, 9869
Chertok, I. M. 1982, Geomagn. Aeron., 22, 182
Chertok, I. M., & Gnezdilov, A. A. 1993, Pis'ma Astron. Zh., 19, 73
Chertok, I. M., et al. 1991, Proc. 3d COSPAR Colloq. 607
Cliver, E. W., et al. 1985, J. Geophys. Res., 90, 6251
———. 1999, Sol. Phys., 187, 89
Delannee, C., et al. 2000, A&A, 355, 725
Dougherty, B. L., et al. 2000, in ASP Conf. Ser. 206, High Energy Solar Physics—Anticipating HESSI, ed. R. Ramaty & N. Mandzhavidze (San Francisco: ASP), 367
Dulk, G. A. 1985, ARA&A, 23, 169
Gary, D. E. 1985, ApJ, 297, 799
Gergeley, T. E. 1986, Sol. Phys., 104, 175
Gilbert, H. R. 2000, ApJ, 537, 503
Gopalswamy, N., & Thompson, B. J. 2000, J. Atmos. Sol.-Terr. Phys., 62, 1457
Gosling, J. T. 1993, J. Geophys. Res., 98, 18937
Gosling, J. T., et al. 1976, Sol. Phys., 48, 389
Harrison, R. A. 1995, A&A, 304, 585
Harrison, R. A., et al. 1990, J. Geophys. Res., 95, 917
Holt, S. S., & Ramaty, R. 1969, Sol. Phys., 8, 119
Hudson, H. S., & Cliver, E. W. 2001, J. Geophys. Res., 106, 25199
Hudson, H. S., et al. 1998, Geophys. Res. Lett., 25, 2481
Kahler, S. W. 1982, J. Geophys. Res., 87, 3439
———. 1989, ApJ, 344, 1026
Kocharov, L., et al. 2001, A&A, 370, 1064
Kundu, M. R. 1965, Solar Radio Astronomy (New York: Wiley)
Kundu, M. R., et al. 1994, ApJS, 90, 599
Low, B. C. 1996, Sol. Phys., 167, 217
Lu, E. T., & Petrosian, V. 1989, ApJ, 338, 1122
MacQueen, R. M., & Fisher, R. R. 1983, Sol. Phys., 89, 89
Marsh, K. A., & Hurford, G. J. 1982, ARA&A, 20, 497
Moreton, G. E., & Ramsey, H. E. 1960, PASP, 72, 357
Moses, D., et al. 1997, Sol. Phys., 175, 571
Munro, R. H., et al. 1979, Sol. Phys., 61, 201
Neupert, W. M. 1968, ApJ, 153, L59
Nita, G. M., Gary, D. E., Lanzerotti, L. J., & Thomson, D. J. 2002, ApJ, 570, 423
Robinson, R. D., & Stewart, R. T. 1985, Sol. Phys., 97, 145
Robinson, R. D., et al. 1986, Sol. Phys., 105, 149
Sheeley, N. R., et al. 1975, Sol. Phys., 45, 377
———. 1983, ApJ, 272, 349
St. Cyr, O. C., & Webb, D. F. 1991, Sol. Phys., 136, 379
St. Cyr, O. C., et al. 1999, J. Geophys. Res., 104, 12493
———. 2000, J. Geophys. Res., 105, 18169
Vrsnak, B., et al. 1995, Sol. Phys., 158, 331
Webb, D. F. 2000, J. Atmos. Sol.-Terr. Phys., 62, 1415
Webb, D. F., & Howard, R. A. 1994, J. Geophys. Res., 99, 4201
Webb, D. F., & Hundhausen, A. J. 1987, Sol. Phys., 108, 383